Spectroscopic studies of nile red in organic solvents and polymers

Ashim Kumar Dutta, Kenji Kamada, Koji Ohta *

Photonic Chemistry Section, Department of Optical Materials, Osaka National Research Institute, AIST, Ikeda, Osaka 563, Japan

Abstract

We have studied the spectroscopic properties of nile red (NR), a highly fluorescent laser dye, in organic solvents, binary solvent mixtures and polymers. Spectroscopic studies reveal remarkable changes in the absorption and emission band positions and intensities as a function of the polarity of the medium. Such large changes have been attributed to the twisted intramolecular charge transfer (TICT) state of the molecule in polar medium. Experimental results show that the molecule is sensitive to the polarity of its microenvironment and is an excellent probe for systems presenting restricted geometries. We have incorporated NR into thin films of poly(methyl methacrylate) (PMMA) and poly(vinyl alcohol) (PVA); it is found that the micropolarity in PVA is greater than that in PMMA; in PVA, the micropolarity corresponds to that of a binary mixture of acetonitrile and water, whereas in PMMA, the micropolarity corresponds closely to that of pure acetonitrile.

Keywords: Nile red; Twisted intramolecular charge transfer (TICT) states; Steady state fluorescence; Time-resolved fluorescence; Aggregation-induced dual fluorescence

1. Introduction

Organic polymers have largely replaced conventional materials due to their high durability, transparency and processability, even at the molecular level, which makes them extremely suitable for optoelectronic and microelectronic devices. Moreover, the non-linear optical response of organic materials doped in polymers and their direct application in information processing systems have made the study of dyes doped in polymers of interest in recent years.

Although studies on organic fluorescent dyes incorporated into polymers and glasses have been performed, little information is available on the nature of the interaction between the dye and its microenvironment. Various factors, such as the pore size, polarity, hydrogen bonding and other specific interactions, may be responsible for changes in the photophysical behaviour of dye molecules doped into such systems. Recent studies [1–3] have identified certain fluorophores which specifically sense a particular aspect of the microenvironment, but are unaffected by other factors. Spectroscopic studies of such specific dye molecules and investigations of the energy and electron transfer processes in various systems presenting restricted geometries, namely cyclodextrins [4], micelles [5,6], silica gels [7,8], clays [9,10], polymer latexes [11,12], Langmuir–Blodgett (LB)

films [13,14], microparticles [15,16] and zeolites [17,18], have provided information on the role of the topology of these systems in controlling the photophysical properties of the probe molecules.

More interesting results are expected for molecules which are themselves very flexible and sense the microenvironment in which they are located. Such possibilities are offered by molecules which undergo configurational changes when subjected to pressure or when encapsulated in pores or vessels where free movement is restricted. Molecules exhibiting twisted intramolecular charge transfer (TICT) properties [19–21] are ideal for such purposes and can be profitably utilized to sense the effects of changes in the microcavity due to external influences such as temperature, pressure, etc. [22]. Recently, several aminobenzoic acid derivatives [23] exhibiting TICT characteristics have been employed to study the effects of polarity and free volume in polymers.

In this work, we report the spectroscopic properties of nile red (NR), a highly fluorescent laser dye, in various solvents and polymers. The strong dependence of the absorption and emission band maxima on the polarity of the solvent indicates that the molecule is highly sensitive to the polarity of the medium in which it is located. The spectroscopic studies suggest that the polarity dependence of the NR molecules may be explained in terms of TICT processes; this is possible due to the presence of the flexible diethylamino end group attached to the otherwise rigid structure of the molecule.

---

* Corresponding author.

Moreover, we have established that NR may be used as a probe molecule to estimate the micropolarity in polymer thin films using steady state luminescence spectroscopy.

2. Experimental details

NR (Aldrich Chemical Co., USA) was used as received. The purity of the sample was checked using thin layer chromatography and absorption and emission spectroscopy. All solvents used were of spectroscopic grade (Dojin Chemical Co., Japan). The polymers poly(methyl methacrylate) (PMMA) and poly(vinyl alcohol) (PVA) were obtained from Mitsubishi Rayon Co. (Japan) and Nakarai Chemicals Ltd. (Japan) respectively and were used after purification. The polymers were purified by dissolution in appropriate solvents and reprecipitation from methanol. Doping of the polymers was achieved by mixing appropriate amounts of the dye in a common solvent (stirring well for a prolonged period of time to ensure homogeneous mixing), and thin films were obtained by the spin coating method using a spin coater unit (Mikasa 1H-DX11, Japan). The films were allowed to dry in a vacuum oven for about 24 h and then washed with ethanol to remove NR sticking to the surface of the films. Washing was continued until the last traces of the dye had disappeared, which was ascertained from the absorption spectra of the washings. Ethanol was used to wash PMMA films and chloroform was used to wash PVA films to ensure minimal damage. Finally, the films were dried in a vacuum oven at a temperature of approximately 80 °C for a period of about 5 days to ensure no trace of the solvents remained. The absorption and emission spectra of the films were recorded using a Shimadzu 2200 UV absorption spectrophotometer and a Hitachi F-3010 fluorescence spectrophotometer respectively. The emission from the films deposited on quartz plates was recorded by placing the films in suitable holders which were inclined at an angle of 45° to the incident beam. Suitable narrow bandpass filters were used to eliminate contributions from the scattering of the incident beam from the surface of the films. Fluorescence lifetime measurements were performed on a Horiba NEAS 1100 nanosecond spectrofluorometer using a pulsed hydrogen lamp with a pumping frequency of 10 Hz and a full width at half-maximum (FWHM) of about 0.5 ns. The fluorescence decay profiles were analysed using single- or multi-exponential software programs obtained from Horiba.

3. Results and discussion

3.1. Spectroscopic studies of NR in hexane and carbon tetrachloride

The absorption and emission spectra of NR in hexane and carbon tetrachloride are shown in Figs. 1(a) and 1(b). In hexane (Fig. 1(a)), the absorption profile in the spectral
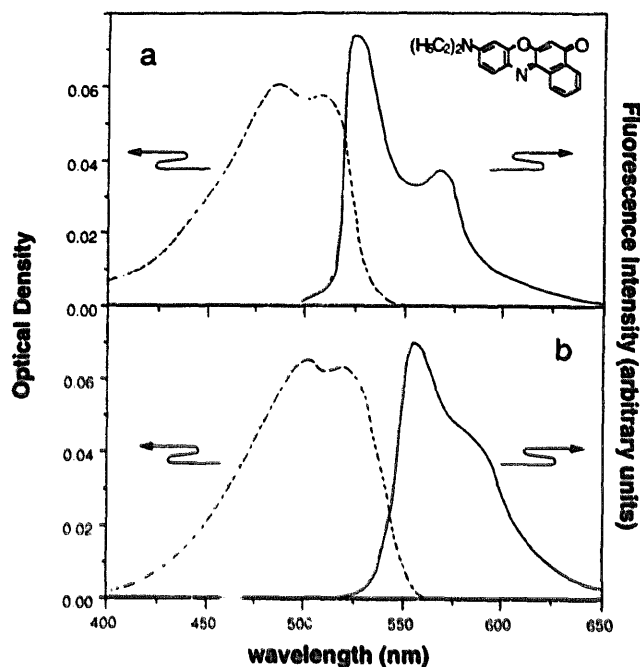

Fig. 1. (a) Absorption (broken line) and emission (full line) spectra of NR $(2.51 \times 10^{-6}$ M) in hexane. (b) Absorption (broken line) and emission (full line) spectra of NR $(1.88 \times 10^{-6}$ M) in carbon tetrachloride.

range 400–600 nm is broad and diffuse with two band maxima, one at 488 nm and the other at 508 nm. The steady state room temperature emission spectrum in the spectral region 500–800 nm is also broad with two distinct band maxima at 525 and 570 nm. The substantial overlap between the absorption and emission spectra of NR in hexane indicates that there is no or little distortion of the molecules in the excited state in this solvent. Fig. 1(b) shows the absorption and emission spectra of NR in carbon tetrachloride at room temperature. The absorption spectrum in the region 400–600 nm shows two distinct bands at 500 and 522 nm and the emission spectrum in the region 500–800 nm shows similar bands at 555 and 585 nm. The red shift of the absorption and emission bands in carbon tetrachloride relative to those in hexane may be attributed to the slightly greater polarity of carbon tetrachloride than hexane. The red shift of the bands and their comparatively smaller overlap in carbon tetrachloride suggest that the molecules are strongly sensitive to the polarity of their microenvironment. To investigate the origin of the two bands in the absorption and emission spectra, the excitation spectra and lifetimes monitored at the two emission band maxima were recorded. The identical nature of the excitation spectra and lifetimes (data not shown) monitored at the emission band maxima clearly indicates that the bands originate from the same electronic state and are probably vibronic.

3.2. Spectroscopic studies of NR in polar solvents

In order to study the role of the polarity in modifying both the ground and excited states of the molecule, we investigated the absorption and emission characteristics of NR in various
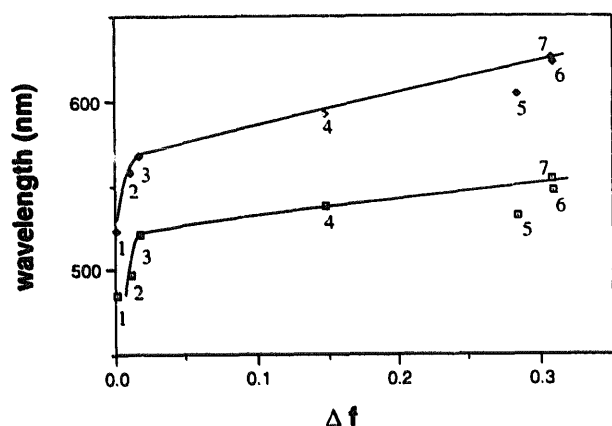
Fig. 2. Plot of absorption (bottom curve) and emission (top curve) band maxima positions of NR in different solvents vs. Δf of the solvents: (1) hexane; (2) CCl_4; (3) toluene; (4) $CHCl_3$; (5) acetone; (6) ethanol; (7) methanol.

pure solvents of different polarity [24]. Fig. 2 shows a plot of the positions of the absorption and emission band maxima vs. the solvent parameter Δf for different pure solvents. The values of Δf were calculated using Eq. (1b) (see below). The dielectric constants (ϵ) and refractive indices (n) of the pure solvents were obtained from Ref. [25a]. The large shift in the absorption and emission band maxima with increasing polarity of the solvent indicates that the excited state of the molecule experiences a more polar environment than the ground state. A convenient method of estimating changes in the dipole moment of the molecule as a result of excitation is the Mataga–Lippert equation [26]

$$\Delta \nu = \nu_{max}^{abs} - \nu_{max}^{em}$$

$$= \frac{2}{cha^3} \Delta f(\mu^* - \mu)^2 + \text{constant} \tag{1a}$$

where

$$\Delta f = \frac{\epsilon - 1}{2\epsilon + 1} - \frac{n^2 - 1}{2n^2 + 1} \tag{1b}$$

According to this equation, $\Delta \nu$ is the difference between the absorption and emission energies, ϵ and n are the dielectric constant and refractive index of the medium respectively, μ^* and μ are the dipole moments of the molecule in the excited and ground states respectively and a is the radius of the cavity surrounding the molecule. From the absorption and emission spectra recorded for various solvents with a wide range of ϵ and n values, and assuming the magnitude of a to be approximately 5 Å [27], the value of the difference ($\mu^* - \mu$) was obtained as about 6.8 D, which is in good agreement with the findings of other workers [24,27,28]. Such a large change in the excited state dipole moment of the molecule seems to suggest corresponding large changes in the excited state configuration. One possible cause could be the geometrical distortion of the molecule in the excited state.

In this context, it should be noted that dimethylaminobenzonitrile (DMABN) [29,30], arylanilines [31,32] and

rhodamine derivatives [33–36] show similar behaviour in polar solvents. Such observations have been accounted for in terms of the TICT process [19–21,29–36]. According to this model, on electronic excitation, the molecule initially forms a moderately non-polar state with a geometry similar to that in the ground state. The transfer of an electron from an electron donor to an electron acceptor group results in a twisted configuration of the molecule, in which the donor and acceptor groups are oriented almost perpendicular to each other. Such a twist usually results in a lowering of the activation barrier, which decreases linearly with increasing polarity of the solvent [19–21,37]. A close examination of the molecular structure of NR, shown in the inset of Fig. 1(a), reveals that the small electron donor group ($(C_2H_5)_2N$, connected to the rigid aromatic electron withdrawing system by a single bond, makes free rotation about the bond possible. It is therefore plausible that TICT may give rise to large shifts in polar medium. Furthermore, the fluorescence quantum yield (Φ_f) and fluorescence lifetime (τ_f) decrease with increasing polarity of the solvent, i.e. increasing Δf values as shown in Table 1. The decreasing values of the radiative decay constant (K_r) and the corresponding increasing values of the non-radiative constant (K_{nr}) clearly suggest that TICT is the principal process responsible for the observed changes.

The similar red shifts observed in the absorption and emission bands over a very wide range of solvents rule out the possibility of any specific interactions, such as hydrogen bonding, etc. To investigate the role of aggregation (if any), we studied the absorption, emission and excitation spectra of NR in different solvents over a very large range of concentration. In this context, it should be noted that most dye molecules, e.g. rhodamines, show evidence of aggregation, involving the manifestation of new structures in their absorption bands and the quenching of the fluorescence emission due to efficient energy transfer from the monomeric species (of rhodamine) to the non-fluorescent dimeric species [3].

Table 1
Fluorescence characteristics of NR[f] in different solvents [g]

Solvent	Δf	Φ_f[a,c]	τ_f[b] (ns)	χ^2[e]	K_r[b,d] ($\times 10^{-7}$ s^{-1})	K_{nr}[b,d] ($\times 10^{-7}$ s^{-1})
CCl_4	0.011	0.65	5.12	1.08	12.62	6.91
$CHCl_3$	0.148	0.33	4.32	1.17	7.69	15.45
Acetone	0.284	0.32	4.66	0.98	7.02	14.88
Acetonitrile	0.304	0.29	4.57	0.89	6.11	15.34
Ethanol	0.308	0.12	3.60	1.22	3.43	24.34
Methanol	0.309	0.08	3.59	1.08	2.11	25.74

[a] Quantum yield was determined with respect to that of rhodamine 6G in ethanol as 0.95.
[b] K_r and K_{nr} correspond to the radiative and non-radiative rate constants and τ_f is the fluorescence lifetime.
[c] $\Phi_f = K_r\tau_f$.
[d] $K_r + K_{nr} = \tau_f^{-1}$.
[e] χ^2 corresponds to the residuals of the best-fit curves for the single-exponential fluorescence decay profiles.
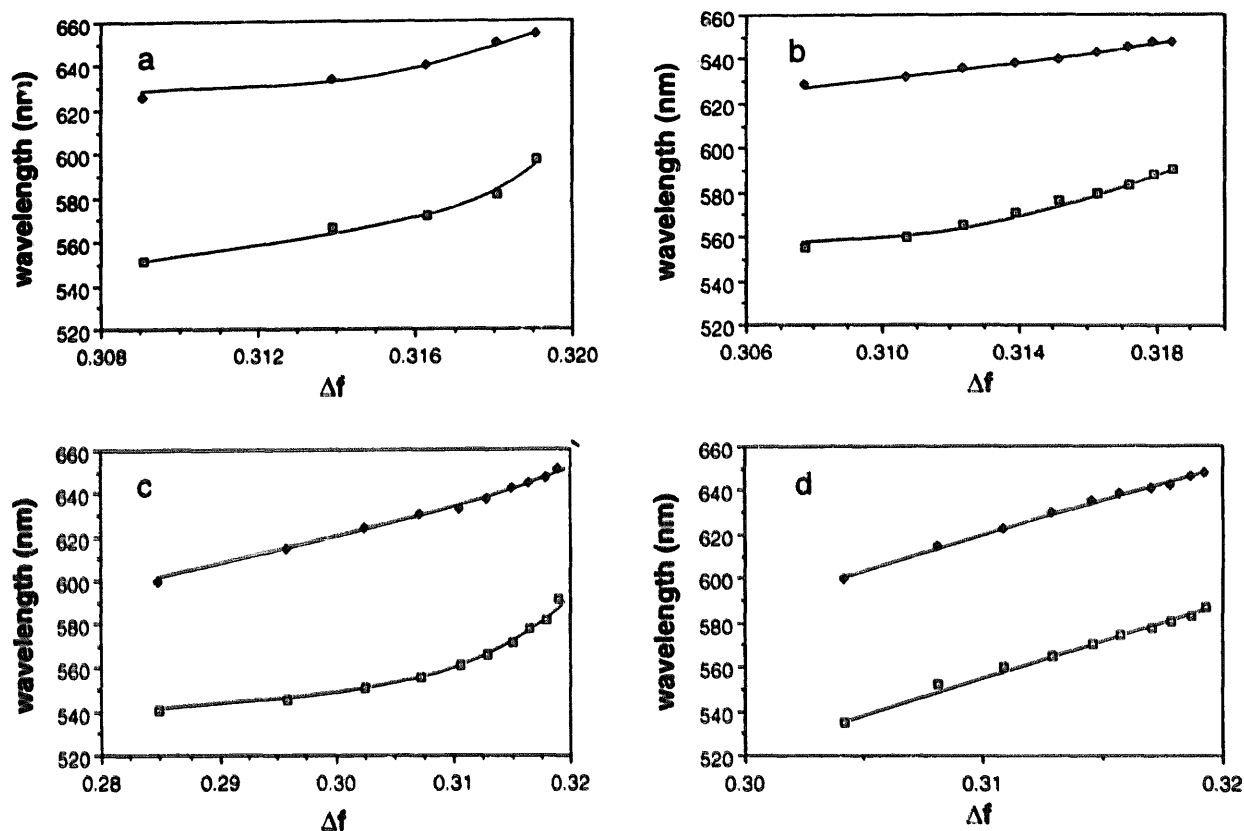[f] Concentration of NR was 2.2×10^{-5} M.
[g] Excitation at 500 nm.

Fig. 3. Plot of absorption (bottom curve) and emission (top curve) band maxima positions vs. Δf values of binary mixtures of water and different hydrocarbons: (a) ethanol; (b) methanol; (c) acetone; (d) acetonitrile.

With increasing concentration of NR in different solvents, the emission intensity increased. Moreover, the absence of new structures in the absorption and emission spectra with increasing concentration of NR suggests that the contribution from aggregates of the dye molecules in solution is negligible.

To pursue further the role of polarity, we used binary solvent mixtures to vary the polarity continuously between two extreme values corresponding to the polarities of the two pure solvents. The solvent–water combinations used were methanol–water, acetonitrile–water, acetone–water and ethanol–water. Figs. 3(a)–3(d) show the absorption and emission band positions of NR vs. Δf at different compositions of the solvent–water mixtures. The Δf values were calculated from the dielectric constants (ϵ) and refractive indices (n) of the different volume compositions of the solvent–water mixtures [25b]. The absorption and emission band positions shift towards the red with increasing Δf values, i.e. increasing volume fraction of water in the binary solvent–water mixtures, similar to the shifts observed in pure solvents with increasing values of Δf. Figs. 4(a)–4(d) show a decrease in the normalized intensity of the emission bands of NR with increasing values of Δf of the binary solvent mixtures (i.e. increasing volume fraction of water), which is in accordance with the findings of other workers [19,24]. This result is also consistent with the decrease in the quantum yield of fluorescence in the pure solvents (Table 1) and supports the hypoth-

esis of polarity-dependent TICT processes in NR. With increasing polarity, the activation barrier of the TICT process decreases. This results in an increase in the rate of non-radiative processes to the triplet state, which is manifested as a decrease in the quantum yield of emission of the molecules in highly polar medium.

Perhaps the most convincing evidence for TICT properties in NR is obtained from the emission and excitation spectra of NR in methanol and methanol–water mixtures, shown in Figs. 5 and 6. Fig. 5 shows the emission spectra of NR in pure methanol (band maximum, 625 nm) and methanol–water (band maxima, 585 and 645 nm). Increasing the volume fraction of water in the binary mixture leads to a change in the intensity ratio of the bands, indicating that the bands do not represent vibronic states but possibly originate from different electronic states. The excitation spectra (Fig. 6) monitored at the emission maxima of 585 and 645 nm reveal two distinct peaks at 530 and 600 nm respectively. Such a large difference indicates that the bands originate from completely different species or configurational states, which is in agreement with the TICT model. We also measured the fluorescence lifetimes of the emissions monitored at 585 and 645 nm. A deconvolution program for multicomponent analysis was initially used to analyse the decay profile. The results obtained show that the major contribution comes from the first component of the multicomponent series, while the con-
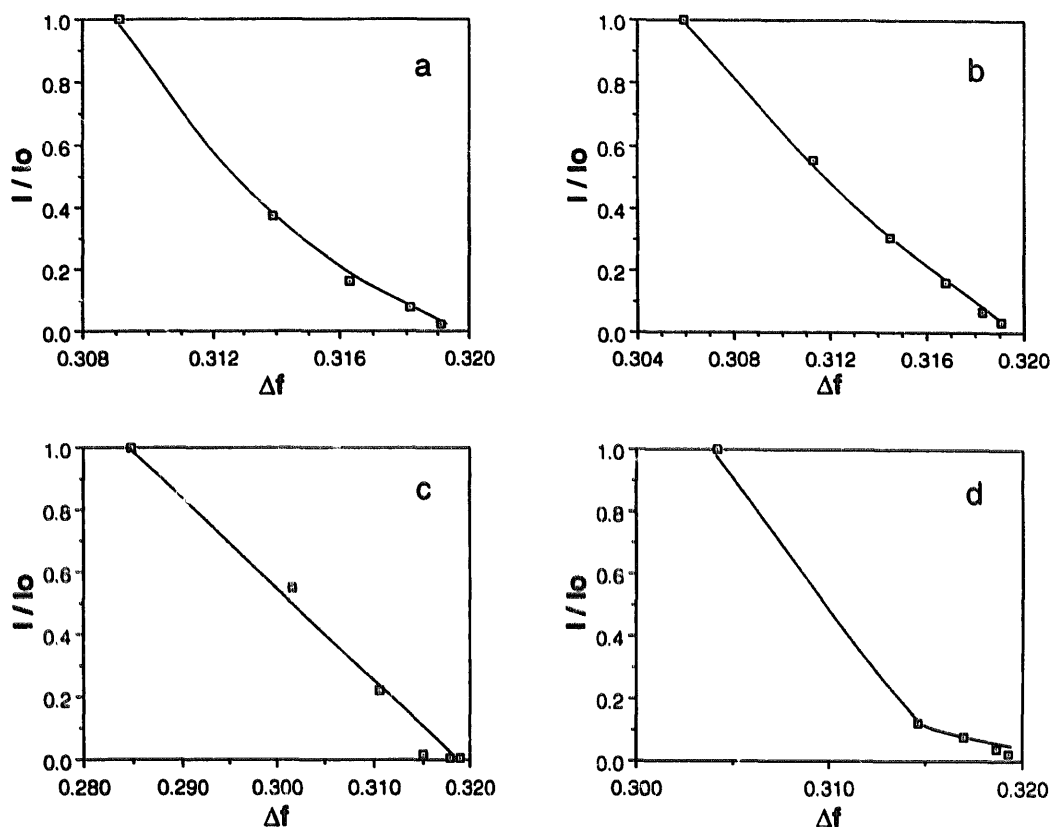
Fig. 4. Plot of the normalized intensity of emission of NR vs. Δf values of the binary mixtures of water and hydrocarbon: (a) ethanol; (b) methanol; (c) acetone; (d) acetonitrile. I is the intensity of emission of NR in the binary solvent mixture of hydrocarbon and water and I_o is the intensity of an equivalent amount of NR in the pure hydrocarbon used in the mixture.
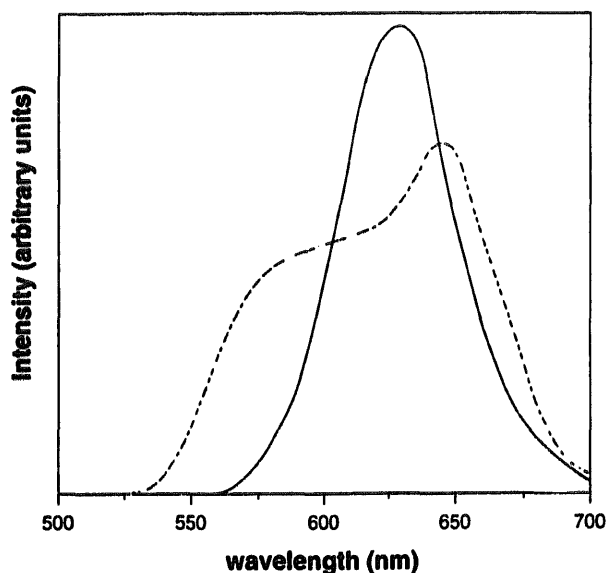

Fig. 5. Emission spectra of NR in pure methanol (full line) and in a binary mixture (broken line) of 90 vol.% water and 10 vol.% methanol.
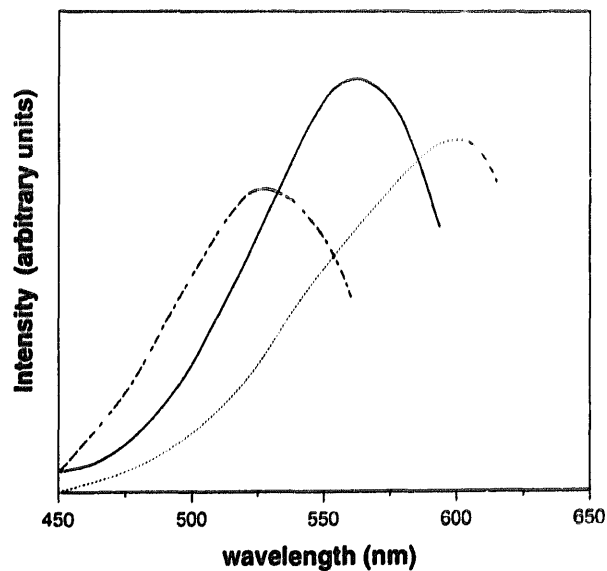

Fig. 6. Excitation spectra of NR in pure methanol with an emission maximum at 625 nm (full line) and in a binary mixture of 10 vol.% methanol and 90 vol.% water with the emission maxima at 585 nm (broken line) and 645 nm (dotted line).

tribution from the other components is almost negligible. Using a single-exponential analysis program, good fits with the experimental data are obtained. The lifetimes obtained for the bands at 585 and 645 nm are 1.56 ± 0.03 ns and 0.92 ± 0.05 ns respectively. The χ^2 values, which measure

the reliability of the best fits obtained, are 1.23 and 1.68 respectively. The distinct differences between the band positions of excitation and emission and between the lifetimes of
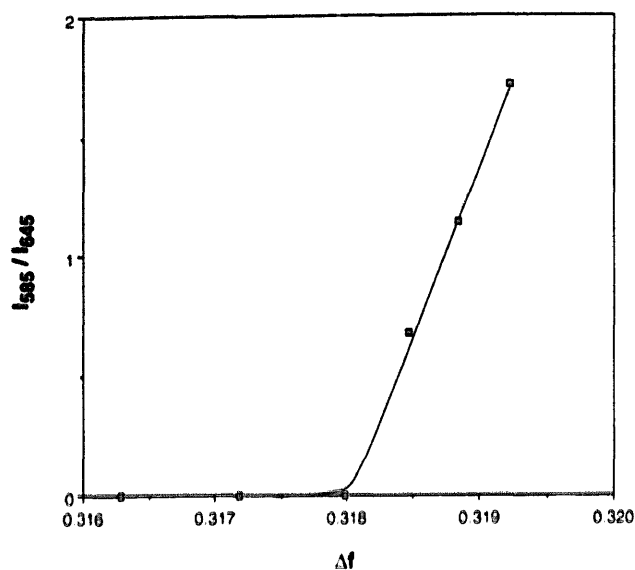
Fig. 7. Plot of I_{585}/I_{645} vs. Δf.

the two bands provide compelling evidence that the two states are indeed different.

Fig. 7 shows a plot of the intensity ratio of the emission bands at 585 and 645 nm vs. Δf of the methanol–water mixture. With increasing Δf values (i.e. increasing volume fraction of water in the mixture), it can be seen that the I_{585}/I_{645} ratio increases sharply above a critical concentration corresponding to $\Delta f = 0.318$. Although such a behaviour seems inexplicable, it is possible that, with increasing amounts of water in the binary mixture, the hydrophobic interaction between NR and water molecules increases. Moreover, the solubility of NR in the mixture also decreases, as NR is almost insoluble in water, resulting in the aggregation of NR molecules. It is plausible that organized aggregates are formed in the binary solvent mixtures, which probably affect the energy transfer process from one configurational state, corresponding to the band at 585 nm, to the other, corresponding to the band at 645 nm, giving rise to dual fluorescence. The existence of organized aggregates in aqueous solutions has been reported for several dye molecules [38]. The fact that the intensity ratio of the 585 and 645 nm bands increases with increasing volume fraction of water readily supports the suggested mechanism. In this context, it should be noted that, in pure methanol, no new bands are observed even for very high concentrations of NR. Although the aggregation of dye molecules in methanol most certainly exists [3], it is probable that these aggregates are randomly organized and do not produce any large changes in the exciton band or in the spectrum. Furthermore, other pure solvents in which NR is readily soluble, that have Δf values equivalent to that of a methanol–water mixture containing 80% or more of water, do not exhibit the band at 585 nm. These preliminary results indicate that, although two energetic states are generated as a result of the TICT character of the molecule in a polar microenvironment, their manifestation as dual fluorescence is induced by the organized aggregates formed in the binary

solvent–water mixture, which seem to affect the energy transfer efficiency from the higher configurational state to the lower.

3.3. Utilization of NR as a molecular probe to estimate and compare the polarity of microenvironments in PMMA and PVA films

In an attempt to estimate the micropolarity in polymers, we incorporated NR dye molecules in PMMA and PVA. Figs. 8(a) and 8(b) show the absorption and emission spectra of NR doped in PMMA and PVA matrices. The absorption spectrum of NR doped in a PMMA matrix shows a broad band in the 500–600 nm region with a band maximum at about 535 nm. The emission band is broad and diffuse with a maximum at around 600 nm. In a PVA matrix, the absorption band is broad and diffuse with a maximum at around 580 nm and the corresponding emission band is located at 600 nm. The excitation spectra, monitored at the emission maxima in PMMA and PVA, show distinct bands at around 535 and 580 nm respectively, which are in good agreement with the reported absorption spectra and confirm the genuine nature of the emission bands obtained in the two polymers.

It is well established that large empty spaces exist between the long chains or coils in polymers; small molecules such as NR (length, 10 Å; width, 7 Å) may be easily incorporated into such spaces and are therefore appropriate to probe the microenvironment. Recent studies have revealed that the
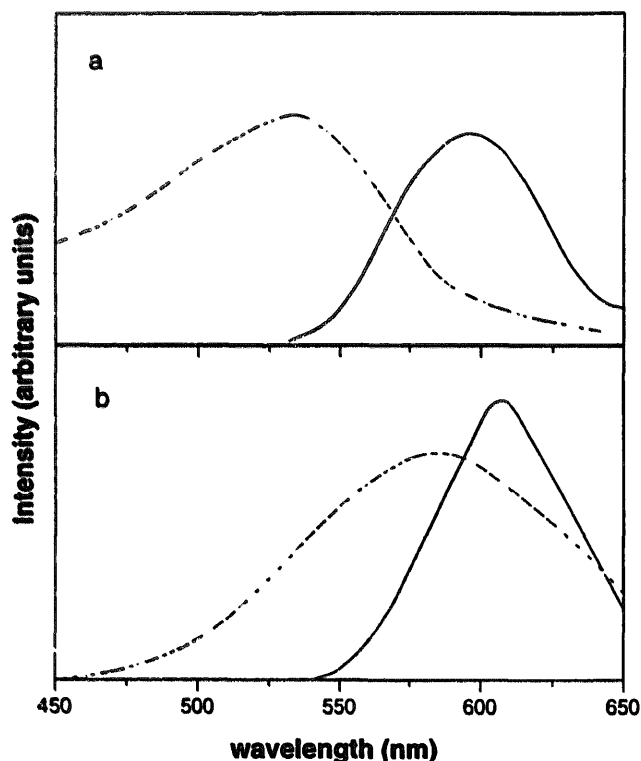

Fig. 8. (a) Absorption (broken line) and emission (full line) spectra of NR in PMMA films. (b) Absorption (broken line) and emission (full line) spectra of NR in PVA films.

microenvironment in restricted geometries, namely zeolites, closely corresponds to that of binary mixtures of an organic solvent and water [39,40]. It is therefore tempting to compare the micropolarity in these polymers to that of binary solvent–water mixtures. Since the emission bands in both PMMA and PVA are located at about 600 nm, we have chosen to use the absorption band positions to obtain a measure of the polarity. Comparing the absorption band maxima obtained in the polymers with those observed in binary acetonitrile–water mixtures (Fig. 3(d)), it can be seen that the polarity in PMMA corresponds to that of pure acetonitrile, whereas that in PVA corresponds to a mixture containing 30% acetonitrile and 70% water. This result clearly demonstrates that PMMA is much less polar than PVA [41]. The fluorescence lifetime of NR in PMMA is 3.67 ns, whereas that in PVA is much shorter (about 1.57 ns). The decay profiles are single exponentials having χ^2 values of 1.06 and 1.46 in PMMA and PVA respectively. These results confirm that the microenvironment in a PVA matrix is much more polar than that in a PMMA matrix. In this context, it should be noted that the ratio of the first and third vibronic bands in pyrene has been adopted as a measure of micropolarity (referred to as the Ham effect in Ref. [42]) and has been effectively employed to estimate the polarity in such diverse situations as solutions [42] and Langmuir films [43]. It seems possible that NR may be used as an efficient polarity-sensitive probe to measure and compare the micropolarity in different polymers. Furthermore, the sharp changes in the spectral properties of NR with small changes in polarity may be profitably utilized in designing humidity sensors.

4. Conclusions

These preliminary studies have established that NR is highly sensitive to the polarity of the microenvironment in which it is located. The large shifts in the absorption and emission bands may be attributed to large changes in the excited state dipole moment of the molecule brought about by polarity-dependent TICT processes. Moreover, quantum yield measurements and time-resolved studies have established that, with increasing polarity and hence TICT effects, the fluorescence quantum yield and radiative decay components decrease, whereas the non-radiative components increase; these are essentially the characteristic features of TICT processes. Furthermore, our results illustrate that, although two configurational states are generated due to TICT, efficient energy transfer from the higher configurational energy state to the lower leads to strong fluorescence from the lowest energy state giving rise to a single broad-band spectrum. However, in binary solvent–water mixtures, organized aggregates are formed due to interaction of the NR molecules with their microenvironment and the self-assembling characteristics of the molecules. This organized aggregation of the molecules may impede energy transfer from the energetically higher TICT state to the lower state, resulting

in dual fluorescence. We have also used NR as a molecular probe to determine the micropolarity within polymers. Our results reveal that the micropolarity in PMMA is much less than that in PVA. Indeed, the micropolarity of PVA may be compared with that of a binary mixture consisting of 70% water and 30% acetonitrile, whereas the microenvironment in PMMA corresponds to the polarity of pure acetonitrile.

References

[1] K. Kalyansundaram, in V. Ramamurthy (ed.), Photophysics and Photochemistry in Organized and Constrained Media, VCH, New York, 1991, p. 39.

[2] J.M. Loeb, Spectroscopic Membrane Probes, Vols. I–III, CRC Press, New York, 1988.

[3] K.H. Drexhage, in E.P. Schrafer (ed.), Dye Lasers, Springer, New York, 1977, p. 143.

[4] V. Ramamurthy and D.F. Eaton, Acc. Chem. Res., 21 (1988) 300.

[5] K. Kalyansundaram, Chem. Soc. Rev., 7 (1978) 453.

[6] J.K. Thomas, J. Phys. Chem., 91 (1987) 267.

[7] P. Levitz, J.M. Drake and J. Klafter, J. Chem. Phys., 89 (1988) 5224.

[8] J. Klafter, J.M. Drake, P. Levitz, A. Blumen and G. Zumofen, J. Lumin., 45 (1990) 34.

[9] J.K. Thomas, Acc. Chem. Res., 21 (1988) 275.

[10] V.G. Kuykendall and J.K. Thomas, J. Phys. Chem., 94 (1990) 4224.

[11] K. Nakashima, Y.S. Liu, P. Zhang, J. Duhamel, J. Feng and M.A. Winnik, Langmuir, 9 (1993) 2825.

[12] K. Nakashima, J. Duhamel and M.A. Winnik, J. Phys. Chem., 97 (1993) 10 702.

[13] A.K. Dutta, T.N. Misra and A.J. Pal, J. Phys. Chem., 98 (1994) 4365.

[14] A.K. Dutta, T.N. Misra and A.J. Pal, J. Phys. Chem., 98 (1994) 12 844.

[15] K. Kamada, K. Sasaki and H. Masuhara, Chem. Phys. Lett., 229 (1994) 559.

[16] K. Kamada, K. Sasaki, H. Misawa, N. Kitamura and H. Masuhara, Chem. Phys. Lett., 210 (1993) 89.

[17] V. Ramamurthy, Tetrahedron, 42 (1986) 5753.

[18] X. Liu and J.K. Thomas, Chem. Mater., 6 (1994) 2303.

[19] W. Rettig, Angew. Chem. Int. Ed. Engl., 25 (1986) 971.

[20] W. Rettig, in K. Honda (ed.), Photochemical Processes in Organised Molecular Systems, North-Holland, Delta Series, New York, 1991, p. 61.

[21] W. Rettig, in J. Mattay (ed.), Topics in Current Chemistry, Vol. 169, Springer-Verlag, New York, 1994, p. 253.

[22] A.A. Dadali, J.M. Lang and H.G. Drickmayer, J. Photochem. Photobiol. A: Chem., 84 (1994) 203.

[23] K.A. Al-Hassan, J. Photochem. Photobiol. A: Chem., 84 (1994) 207.

[24] G.B. Dutt, S. Doriasamy and N. Periasamy, J. Chem. Phys., 94 (1991) 5360.

[25] (a) R.C. Weast (ed.), Handbook of Chemistry and Physics, CRC Press, Boca-Raton, FL, 1985–1986. (b) The Chemical Society of Japan (ed.), Kagaku Binran Kiso Hen, Vol. 2, Maruzen, Tokyo, 4th edn., 1992 (in Japanese).

[26] J.R. Lacowicz, Principles of Fluorescence Spectroscopy, Plenum, New York, 1983, Chapter III.

[27] N. Sarkar, K. Das, D.N. Nath and K. Bhattacharya, Langmuir, 10 (1994) 326.

[28] D. Reiser and A. Laubereau, Ber. Bunsenges. Phys. Chem., 86 (1982) 101.

[29] Z.R. Gabrowski, K. Rotkiewicz, A. Siemiarczuk, D.J. Cowley and W. Bauman, Nouv. J. Chim., 3 (1979) 443.

[30] K. Rotkiewicz, K.H. Grellmann and Z.R. Gabrowski, Chem. Phys. Lett., 19 (1973) 315.

[31] T. Okada, T. Fujita, M. Kubota, S. Masaki, N. Mataga, R. Ide, Y. Sakata and S. Misumi, Chem. Phys. Lett., 14 (1972) 563.

[32] W. Bauman, F. Petzke and K.-D. Loosen, Z. Naturforsch., Teil A, 34 (1979) 1070.

[33] M. Vogel, W. Rettig, R. Sens and K.H. Drexhage, Chem. Phys. Lett., 147 (1988) 452.

[34] M. Vogel, W. Rettig, R. Sens and K.H. Drexhage, Chem. Phys. Lett., 147 (1988) 461.

[35] M. Vogel, W. Rettig, U. Fiedeldei and H. Baumgartel, Chem. Phys. Lett., 148 (1988) 461.

[36] K.G. Casey and E.L. Quitevis, J. Phys. Chem., 92 (1988) 6590.

[37] J.M. Hicks, M. Vandersall, Z. Barbarogic and K.B. Eisenthal, Chem. Phys. Lett., 116 (1985) 18.

[38] G.J. Tiddy, D.L. Mateur, A.P. Amerod, W.J. Harrisson and D.J. Edwards, Langmuir, 11 (1995) 390.

[39] V. Ramamurthy, D.F. Eaton and J.V. Caspar, Acc. Chem. Res., 25 (1992) 299.

[40] V. Ramamurthy, D.R. Sanderson and D.F. Eaton, Photochem. Photobiol., 56 (1992) 297.

[41] J. Bandrup and E.H. Imergut (eds.), Polymer Handbook, Wiley Interscience, New York, 1989.

[42] K. Kalyansundaram and J.K. Thomas, J. Am. Chem. Soc., 99 (1977) 2039.

[43] E. Wistus, E. Mukhtar, M. Almgren and S.E. Linquist, Langmuir, 8 (1992) 1366.